JOURNAL

OF THE AMERICAN CHEMICAL SOCIETY

VOLUME 110, NUMBER 3 FEBRUARY 3, 1988

Excitation and Dissociation of Isolated Ions Derived from Polycyclic Aromatic Hydrocarbons

Steven J. Pachuta,[†] Hilkka I. Kenttämaa,[‡] Thomas M. Sack,[§] Ronald L. Cerny,[§] Kenneth B. Tomer,[§] Michael L. Gross,*[§] Robin R. Pachuta,[†] and R. Graham Cooks*[†]

Contribution from the Department of Chemistry, Purdue University, West Lafayette, Indiana 47906, and the Midwest Center for Mass Spectrometry, Chemistry Department, University of Nebraska—Lincoln, Lincoln, Nebraska 68588. *Received July 28, 1986*

Abstract: Chemical, electron, and desorption ionization and photoionization, together with photodissociation and high- and low-energy collisional activation, are used to probe the unusual mass spectrometric behavior of polycyclic aromatic hydrocarbons. The extent of fragmentation and even the types of dissociation products are dependent on the activation method used. This is rationalized in terms of energy deposition functions. The method used to deposit energy may also have effects in some cases. Doubly charged and protonated molecules are included in the comparisons made here. Furthermore, parent ions having *different* masses and structures produce common sets of low-mass fragment ions. The similarity in the spectra of different parent ions results from an unusual proclivity for rearrangement after excitation. Extensive rearrangement is favored because the ions studied have high internal energy capacity as indicated by the abnormally large energies required for dissociation. Thus, irreversible ring opening may take place, followed by eliminations of small neutral molecules to form intermediate ions common to many PAH molecules. These ions are suggested to have structures with unbranched cumulated double bonds. Their further fragmentation yields sets of low-mass fragment ions which are common for all parent ions derived from different PAH molecules.

The compounds known collectively as polycyclic aromatic hydrocarbons, PAHs,[1] or polynuclear aromatic hydrocarbons, PNAs, have been studied extensively for decades, primarily because of their often high carcinogenicities and their ubiquity in combustion products.[2] Mass spectrometry has frequently been employed in the analysis of these compounds, but differentiation of isomeric structures has met with limited success.[3] A number of factors are responsible for this difficulty. Electron ionization (EI) of PAHs leads to a minimal amount of fragmentation,[4-9] and that which occurs offers little structural information. Isomers, in particular, give almost identical fragmentation patterns. The same is true for daughter spectra of PAHs obtained by collisional activation.[10-13]

Most ions observed in mass spectrometry arise as the result of fragmentation. Thus, these reactions normally receive considerable emphasis. However, as the activation energy for dissociation increases, isomerization processes become more and more likely. The PAHs are a class of molecules that can accommodate a large amount of internal energy before undergoing fragmentation. It is of interest to inquire into the chemical consequences of this excitation. The difficulty in distinguishing PAH isomers by mass spectrometry suggests that isomerization of the molecular ions accompanies or precedes fragmentation. Similarities in product distributions of many small aromatic ions have been explained on the basis of isomerization and also on the basis of fragmentation via common ionic intermediates.[6,14,15]

The structures of *multiply charged* PAH ions and their dissociation products have been of particular interest. The formation of very abundant doubly charged ions from PAHs upon high-energy collisional activation as well as upon electron ionization indicates the unusual stability of these ions. Experimental results[7,16-18] and theoretical calculations[18,19] provide evidence for

---

[†] Purdue University.

[‡] Purdue University. On leave from the Department of Chemistry, University of Helsinki.

[§] Midwest Center for Mass Spectrometry.

(1) Bjoørseth, A., Ed. *Handbook of Polycyclic Aromatic Hydrocarbons*; Marcel Dekker: New York, 1983.

(2) Freudenthal, R. I.; Jones, P. W., Eds. *Polynuclear Aromatic Hydrocarbons*; Vol. 1 of *Carcinogenesis—A Comprehensive Survey*; Raven Press: New York, 1976.

(3) Simonsick, W. J., Jr.; Hites, R. A. *Anal. Chem.* **1984**, *56*, 2749.

(4) Wacks, M. E.; Dibeler, V. H. *J. Chem. Phys.* **1959**, *31*, 1557.

(5) Wacks, M. E. *J. Chem. Phys.* **1964**, *41*, 1661.

(6) Van Brunt, R. J.; Wacks, M. E. *J. Chem. Phys.* **1964**, *41*, 3195.

(7) Natalis, P.; Franklin, J. L. *J. Phys. Chem.* **1965**, *69*, 2935 and references therein.

(8) Gallegos, E. J. *J. Phys. Chem.* **1968**, *72*, 3452.

(9) Hase, A.; Lin, P. H.; Hites, R. A. In *Polynuclear Aromatic Hydrocarbons*; Freudenthal, R. I., Jones, P. W., Eds.; Vol. 1 of *Carcinogenesis—A Comprehensive Survey*; Raven Press: New York, 1976; p 435.

(10) Shushan, B.; Safe, S. H.; Boyd, R. K. *Anal. Chem.* **1979**, *51*, 156.

(11) Shushan, B.; Boyd, R. K. *Org. Mass Spectrom.* **1980**, *15*, 445.

(12) Shushan, B. I. In *Polycyclic Aromatic Hydrocarbons: Formation, Metabolism and Measurement*; Cooke, M., Dennis, A. J., Eds.; Battelle Press: Columbus, OH, 1983; p 1099.

(13) Zakett, D.; Ciupek, J. D.; Cooks, R. G. *Anal. Chem.* **1981**, *53*, 723.

(14) Rosenstock, H. M.; McCulloh, K. E.; Lossing, F. P. *Int. J. Mass Spectrom. Ion Phys.* **1977**, *25*, 327.

(15) Grotemeyer, J.; Grützmacher, H.-F. *Org. Mass Spectrom.* **1982**, *17*, 353.

0002-7863/88/1510-0657$01.50/0

both linear[7,16,17,19] and cyclic[18] structures for doubly charged ions derived from PAHs.

The development of tandem mass spectrometry (MS/MS)[20] has led to the use of a variety of methods for activating selected ions to induce fragmentation. Examples include collisional activation at high (keV) and low (eV) ion kinetic energies with gaseous targets[20] and with surfaces,[21] photoactivation,[20] and electron impact excitation of ions.[22] New scan types have also been developed for efficient utilization of these methods.[23] The present work takes advantage of these mass spectrometric techniques in a systematic study of the fragmentation of ionized PAHs.

Experimental Section

Conventional EI mass spectra were acquired on a Finnigan 4000 GC/MS. The electron energy was 70 eV, and the ion source temperature was 250 °C. Samples were introduced with use of a direct insertion probe.

High-energy CAD daughter spectra were obtained on two different instruments. All daughter spectra of protonated molecules were acquired with use of a reverse geometry (BE configuration) mass spectrometer which has been described previously.[24] Chemical ionization (CI) was performed with isobutane reagent gas at an ion source pressure of ca. 0.2 Torr. Collision cell pressures sufficient to attenuate the beam by approximately 50% were employed, using air as the collision gas. The accelerating voltage was 7 kV in all experiments. All spectra were signal averaged (5–10 scans) at scan rates of ca. 90 s/scan. The broadness of the peaks in the spectra is the result of two factors: kinetic energy released upon dissociation and the presence of several ions separated by only one mass unit. The peak broadness owing to kinetic energy release is unavoidable when the second stage of mass analysis is performed with an electrostatic (energy) analyzer, as is the case in this study. When a broad peak is actually composed of several peaks, the peak shape is often unsymmetrical, and estimates can be made as to the contribution of individual components to the net peak shape.

High-energy daughter spectra of molecular ions generated by 70-eV EI were acquired with a Kratos MS-50 triple analyzer mass spectrometer (EBE configuration) that has been described previously.[25] The high-resolution front section, of Nier-Johnson geometry, served as the first mass analyzer, while a low-resolution electrostatic analyzer served as the second analyzer. Helium was used as the collision gas to provide approximately 50% beam attenuation in obtaining all daughter and sequential daughter spectra. The accelerating voltage was 8 kV. Sequential daughter spectra[23,26] were obtained by selecting a CAD product formed in the first field-free region and causing it to undergo CAD in the third field-free region. Daughter ion spectra of doubly charged ions formed in the ion source upon 70-eV EI were obtained by setting the accelerating voltage to 4 kV, while keeping all other parameters constant. Doubly charged ions were also generated by charge stripping in the first field-free region with oxygen collison gas; CAD of these ions was carried out in the third field-free region. Typical spectra were the result of signal averaging ten to twenty 20-s scans.

Most of the low-energy CAD experiments were carried out at collision energies of 28 eV or less with a Finnigan TSQ triple quadrupole mass spectrometer.[27] Molecular ions were generated by 70-eV EI, unless otherwise noted. Protonated molecules were generated by CI with isobutane reagent gas at a source pressure of ca. 0.4 Torr, unless otherwise noted. All experiments were performed with argon collision gas at a pressure of ca. 1.7 mTorr in the collision quadrupole, although lower pressures (e.g., 0.1 mTorr) were used to compare the results obtained under single- and multiple-collision conditions. Variation of collision gas pressure was found to have only minor effects on the low-energy CAD spectra of PAH ions.

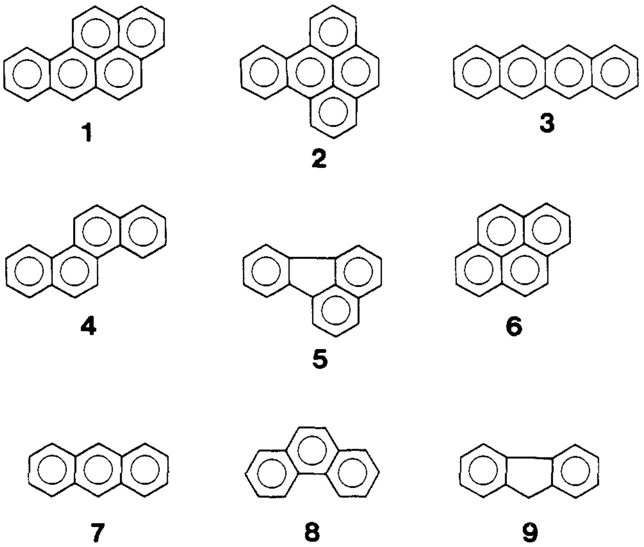

Figure 1. Structures of the PAHs used in this study: **1**, benzo[*a*]pyrene, molecular weight (MW) 252; **2**, benzo[*e*]pyrene, MW 252; **3**, naphthacene, MW 228; **4**, chrysene, MW 228; **5**, fluoranthene, MW 202; **6**, pyrene, MW 202; **7**, anthracene, MW 178; **8**, phenanthrene, MW 178; **9**, fluorene, MW 166.

Some EI and low-energy CAD experiments, as well as all the laser experiments, were performed with a home-built Fourier transform mass spectrometer equipped with a Nicolet FTMS 1000 data system. The instrument is modified for use with a Quanta-Ray DCR-2 Nd:YAG laser operated in the Q-switched mode, and the laser is equipped with a Model HG-2 harmonic generator. The system has been described previously.[28] Samples were introduced into the instrument by deposition from toluene solution onto a probe tip. The probe was held about 20 cm from the ICR cell in a position such that it could be heated by the laser in order to volatilize the sample, but sufficiently remote so that ions formed by desorption from the surface would not enter the cell. EI mass spectra were obtained by using 70-eV electrons (electron beam duration 5 ms) and with a sample pressure of 1×10^{-7} Torr. CAD experiments were performed with argon collision gas at a static pressure of approximately 5×10^{-6} Torr after sample ionization by 10–15-eV electrons. The excitation voltage was pulsed on 1 ms after ionization and remained on for 0.5 to 2 ms. Maximum collision energies were calculated[29] to be about 250 eV. Detection was delayed 50 ms after excitation. Electron impact excitation of ions was accomplished by increasing the duration of the electron beam from 5 to 500 ms at 8–9 eV (nominal). The sample pressures were ca. $1-5 \times 10^{-8}$ Torr. Ionization energy was sufficiently low to assure that fragments were not produced in the ionization event but rather by electron activation.

---

(16) Ast, T.; Beynon, J. H.; Cooks, R. G. *Org. Mass Spectrom.* **1972**, *6*, 749.

(17) Kingston, R. G.; Guilhaus, M.; Brenton, A. G.; Beynon, J. H. *Org. Mass Spectrom.* **1985**, *20*, 406.

(18) Mathur, B. P.; Burgess, E. M.; Bostwick, D. E.; Moran, T. F. *Org. Mass Spectrom.* **1981**, *16*, 92.

(19) Lammertsma, K.; Pople, J. A.; von R. Schleyer, P. *J. Am. Chem. Soc.* **1986**, *108*, 7.

(20) McLafferty, F. W., Ed. *Tandem Mass Spectrometry*; John Wiley & Sons: New York, 1983.

(21) Mabud, M. A.; DeKrey, M. J.; Cooks, R. G. *Int. J. Mass Spectrom. Ion Proc.* **1985**, *67*, 285.

(22) Cody, R. B.; Freiser, B. S. *Anal. Chem.* **1979**, *51*, 547.

(23) Louris, J. N.; Wright, L. G.; Cooks, R. G.; Schoen, A. E. *Anal. Chem.* **1985**, *57*, 2918.

(24) Beynon, J. H.; Cooks, R. G.; Amy, J. W.; Baitinger, W. E.; Ridley, T. Y. *Anal. Chem.* **1973**, *45*, 1023A.

(25) Gross, M. L.; Chess, E. K.; Lyon, P. A.; Crow, F. W.; Evans, S.; Tudge, H. *Int. J. Mass Spectrom. Ion Phys.* **1982**, *42*, 243.

(26) Burinsky, D. J.; Cooks, R. G.; Chess, E. K.; Gross, M. L. *Anal. Chem.* **1982**, *54*, 295.

(27) Slayback, J. R. B.; Story, M. S. *Ind. Res. Dev.* **1981**, February, 129.

(28) Sack, T. M.; McCrery, D. A.; Gross, M. L. *Anal. Chem.* **1985**, *57*, 1290.

(29) Lehman, T. A.; Bursey, M. M. *Ion Cyclotron Resonance Spectrometry*; Wiley-Interscience: New York, 1976.

(30) Wysocki, V. H.; Kenttämaa, H. I.; Cooks, R. G. *Int. J. Mass Spectrom. Ion Proc.* **1987**, *75*, 181.

(31) Levsen, K. *Fundamental Aspects of Organic Mass Spectrometry*; Verlag Chemie: Weinheim, 1978.

(32) Richter, W. J.; Schwarz, H. *Angew. Chem., Int. Ed. Engl.* **1978**, *17*, 424.

(33) Garrison, B. J. *J. Am. Chem. Soc.* **1982**, *104*, 6211.

(34) Kelner, L.; Markey, S. P. *Int. J. Mass Spectrom. Ion Proc.* **1984**, *59*, 157.

(35) (a) Van der Peyl, G. J. Q.; Van der Zande, W. J.; Hoogerbrugge, R.; Kistemaker, P. G. *Int. J. Mass Spectrom. Ion Proc.* **1985**, *67*, 147; (b) de Pauw, E.; Pelzer, G.; Natalis, P. In *Ion Formation from Organic Solids*; Benninghoven, A. D., Ed.; Proceedings of the Third International Conference, Springer Proceedings in Physics; Springer-Verlag: West Berlin, 1986; Vol. 9.

(36) Dunbar, R. C. In *Gas Phase Ion Chemistry*; Bowers, M. T., Ed.; Academic Press: New York, 1979; Vol. 2, p 181.

(37) DeKrey, M. J.; Kenttämaa, H. I.; Wysocki, V. H.; Cooks, R. G. *Org. Mass Spectrom.* **1986**, *21*, 193.

Table I. Techniques Used to Investigate PAH Ions

method	abbreviation	activation independent of ionization	ion lifetime before activation	avg internal energy of activated ions (eV)	assumed shape of internal energy distribution[a]	ref
electron ionization	EI	no	NA[b]	1-5	broad	30, 31
chemical ionization	CI	no	NA	*X*[c]	narrow	20, 32
charge exchange	CE	no	NA	*X*[c]	variable	29
seconday ion mass spectrometry	SIMS	no	NA	1-3	narrow	33-35
multiphoton ionization	MPI	no	NA	0-4	narrow	28
keV collisionally activated dissociation (7 or 8 keV)	CAD, high-energy	yes	<10 μs	1-3	narrow, high-energy tail	20, 30, 36
eV collisionally activated dissociation (10-30 eV, triple quadrupole mass spectrometer)	CAD, low-energy	yes	>10 μs	1-3	variable[d]	29, 36
eV collisionally activated dissociation (<250 eV, Fourier transform mass spectrometer)	CAD, low-energy (FTMS)	yes	1 ms	1-3	variable[d]	29
photodissociation	PD	yes	20 ms	2-5	narrow	36
electron impact excitation of ions	—	yes	variable			21
surface-induced dissociation	SID	yes	≥10 μs	1-8	narrow	37

[a] "Broad" implies a full-width at half maximum (FWHM) of >4 eV; "narrow" implies a fwhm of <4 eV. [b] Not applicable. [c] "X" is determined by thermochemical differences between the reagent ion and the molecule. [d] Depends on collision energy and pressure.

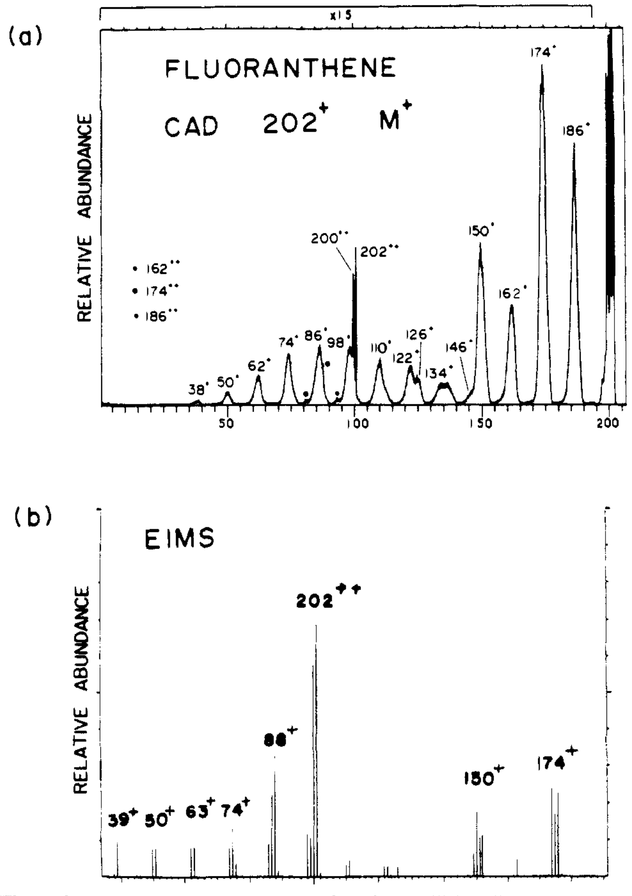

Figure 2. (a) Daughter spectrum produced by collisionally activating the molecular ion $M^{\bullet+}$ (*m/z* 202) of fluoranthene (**5**) at 8 keV (*m/z* values of the peak centroids are labeled). (b) Partial 70-eV EI mass spectrum of fluoranthene.

Laser light of different wavelengths was obtained with use of a harmonic generator (1064-nm fundamental, 532-nm second harmonic, 355-nm third harmonic, and 266-nm fourth harmonic). A UG-11 filter was used at the two shortest wavelengths to remove longer wavelength photons. The laser beam diameter was ca. 0.5 cm in all experiments. The multiphoton ionization (MPI) spectra displaying the most extensive fragmentation were obtained 1064-, 532-, and 266-nm radiation. The best photodissociation results were obtained with pulse energies of 20-50 mJ/pulse at a wavelength of 355 nm, although dissociation products could also be obtained with 1064-nm radiation at energies of 200-400 mJ/pulse. Samples were ionized by 10-15-eV electrons prior to photodissociation. Firing of the laser was delayed 20 ms after the electron beam was shut off.

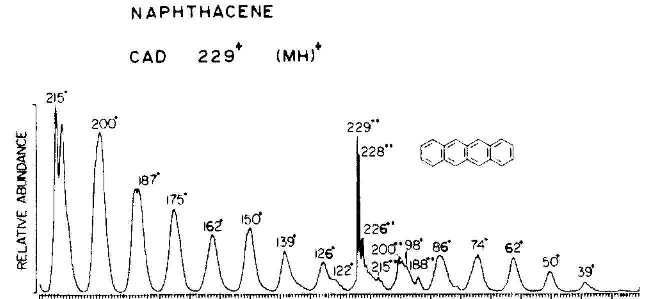

Figure 3. High-energy daughter spectrum of protonated naphthacene (**3**) molecule (*m/z* 229) (*m/z* values of the peak centroids are labeled).

Secondary ion mass spectra were obtained on a Riber SQ156L secondary ion mass spectrometer. Samples were burnished on graphite or platinum substrates and sputtered with 4.0 keV Ar^+ at current densities of $1-10 \times 10^{-9}$ Å cm^{-2}.

The PAH samples (Aldrich) were used as received without further purification.

Results

The compounds studied (Figure 1) include four pairs of isomers. They are all unsubstituted, and the number of rings in each varies from three to five. In addition to the completely unsaturated compounds benzo[*a*]pyrene (**1**), benzo[*e*]pyrene (**2**), naphthacene (**3**), chrysene (**4**), fluoranthene (**5**), pyrene (**6**), anthracene (**7**), and phenanthrene (**8**), a compound with one sp^3 carbon, fluorene (**9**), was included for comparison. The techniques employed to investigate the behavior of gas-phase PAH ions are presented in Table I, together with some important characteristics of these techniques and abbreviations that will be used in this paper. Fragmentation patterns (viz. daughter ion spectra) were recorded for the following ions derived from the PAHs: $M^{\bullet+}$ (the molecular ion), $(M + H)^+$, $(M - H)^+$, $(M - 2H)^{\bullet+}$, $(M - 3H)^+$, $(M - 4H)^{\bullet+}$, $(M - CH_2)^{\bullet+}$, $(M - CH_3)^+$, $(M - CH_4)^{\bullet+}$, $(M - C_2H_2)^{\bullet+}$, M^{2+}, $(M - 2H)^{2+}$, and $(M - C_2H_2)^{2+}$.

In nearly every case, fragmentation indicated by the mass spectra and even the daughter ion spectra was found to be minimal, in agreement with some earlier results.[38-40] The dissociation

---

(38) March, R. E.; Hughes, R. J. *Int. J. Mass Spectrom. Ion Proc.* **1986**, *68*, 167.

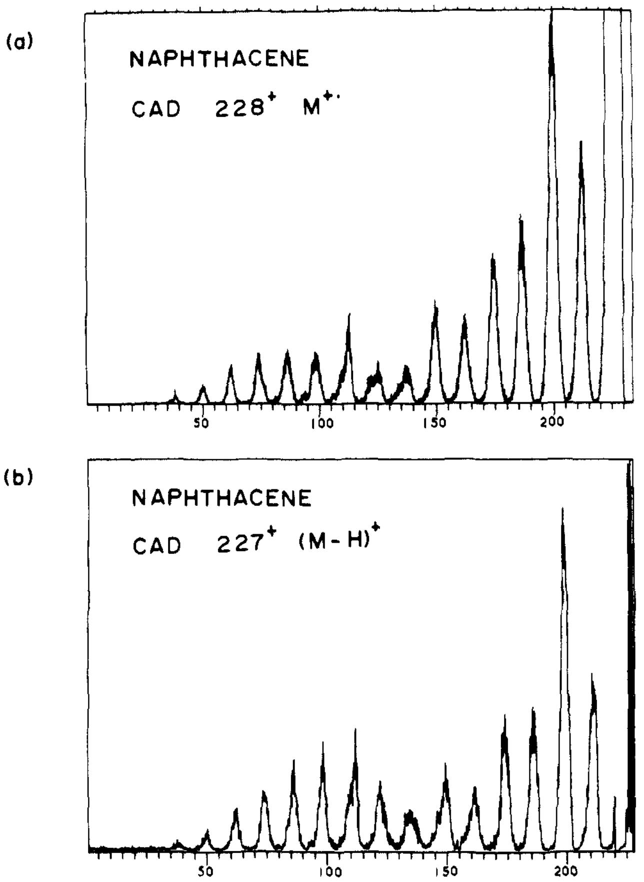

Figure 4. (a) Daughter spectrum produced by collisionally activating the molecular ion $M^{\cdot+}$ (m/z 228) of naphthacene (**3**) at 8 keV. (b) Sequential high-energy daughter spectrum obtained by collisionally activating the $(M - H)^+$ fragment ion (m/z 227) produced by CAD of the naphthacene (**3**) molecular ion $M^{\cdot+}$ (m/z 228).

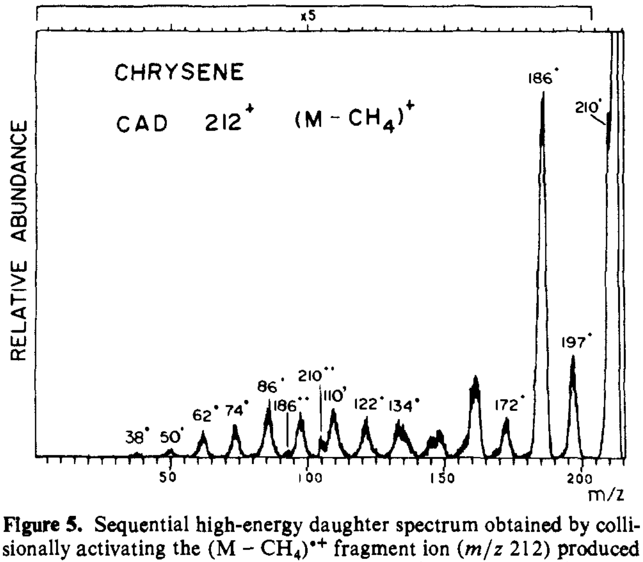

Figure 5. Sequential high-energy daughter spectrum obtained by collisionally activating the $(M - CH_4)^{\cdot+}$ fragment ion (m/z 212) produced by CAD of the chrysene (**4**) molecular ion $M^{\cdot+}$ (m/z 228) (m/z values of the peak centroids are labeled).

patterns obtained for all the different types of ions are remarkably similar. Moreover, the low-mass fragment ion distributions are identical. Spectra typical of those obtained for the various techniques employed are shown in Figures 2–8. Tabulated results can be found in the supplementary material.

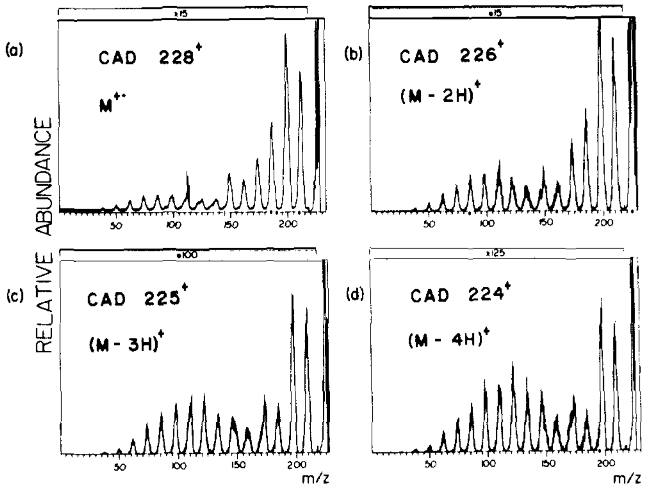

Figure 6. (a) Daughter spectrum produced by collisionally activating the molecular ion $M^{\cdot+}$ (m/z 228) of chrysene (**4**) at 8 keV. (b–d) Sequential high-energy daughter spectra obtained by collisionally activating the $(M - 2H)^{\cdot+}$ ion (m/z 226), the $(M - 3H)^+$ ion (m/z 225), and the $(M - 4H)^{\cdot+}$ ion (m/z 224) produced by CAD of the chrysene molecular ion $M^{\cdot+}$.

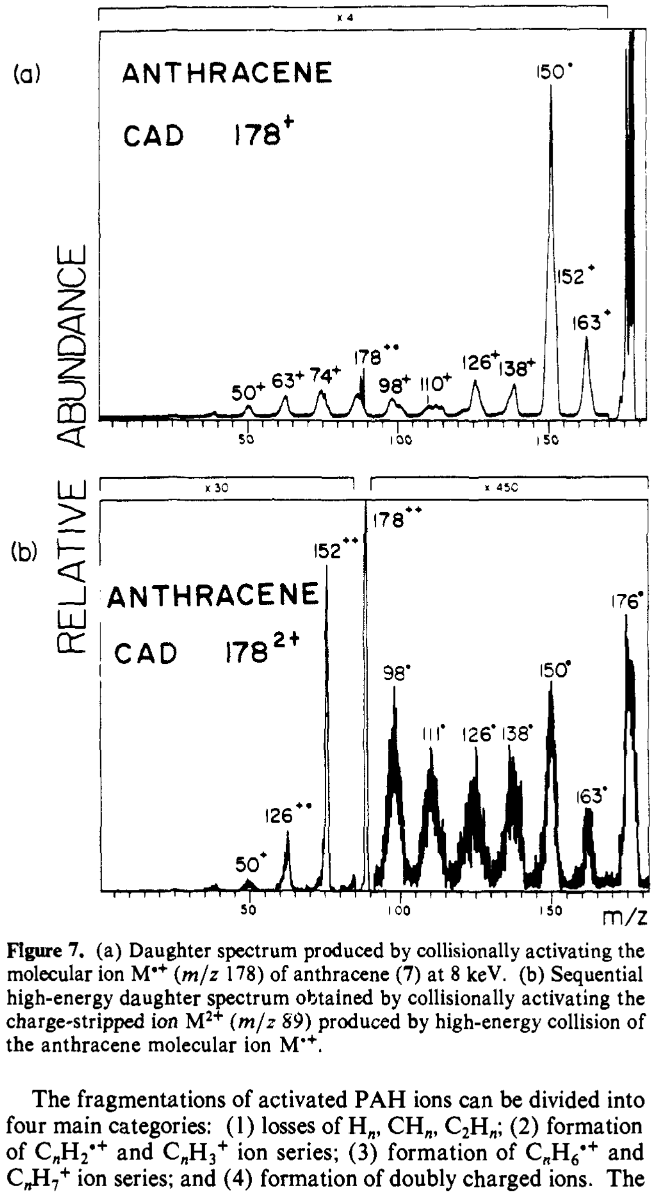

Figure 7. (a) Daughter spectrum produced by collisionally activating the molecular ion $M^{\cdot+}$ (m/z 178) of anthracene (**7**) at 8 keV. (b) Sequential high-energy daughter spectrum obtained by collisionally activating the charge-stripped ion M^{2+} (m/z 89) produced by high-energy collision of the anthracene molecular ion $M^{\cdot+}$.

The fragmentations of activated PAH ions can be divided into four main categories: (1) losses of H_n, CH_n, C_2H_n; (2) formation of $C_nH_2^{\cdot+}$ and $C_nH_3^+$ ion series; (3) formation of $C_nH_6^{\cdot+}$ and $C_nH_7^+$ ion series; and (4) formation of doubly charged ions. The detailed observations relating to these categories are presented below. When possible, the discussion will be centered on chrysene

---

(39) Heller, S. R.; Milne, G. W. A.; Eds. *EPA/NIH Mass Spectral Data Base*; U.S. Government Printing Office: Washington, 1980.

(40) Stenhagen, E.; Abrahamsson, S.; McLafferty, F. W., Eds. *Registry of Mass Spectral Data*; John Wiley & Sons: New York, 1974.

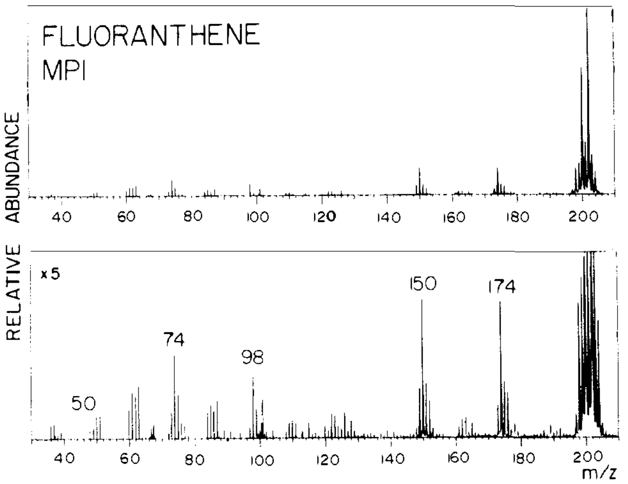

Figure 8. MPI mass spectrum of fluoranthene (5) obtained with combined laser radiation of 1064-, 532-, and 266-nm wavelengths. Pulse energy: ca. 200 mJ/pulse.

Scheme I

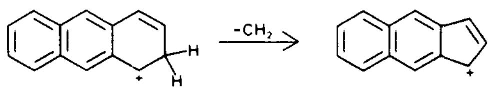

in order to facilitate comparisons.

Losses of H_n, CH_n, and C_2H_n. Losses of H_n typically occur to produce the major fragment ions for all the activation techniques applied in this study.[41] Losses of C_2H_n fragments, particularly C_2H_2 and C_2H_4, are also observed in reasonable abundance (Figures 2–7). With both low- and high-energy collisional activation, the loss of C_2H_n yields the most abundant ion outside of the $(M - H_n)^+$ region for all ions studied (see, for example, Figures 2 and 4–7) except for the protonated PAH molecules in high-energy CAD, fluorene in all experiments, and fluoranthene molecular ion in low-energy CAD. Fragmentation beyond losses of one and two hydrogens and acetylene was not detectable in SIMS experiments (see supplementary material). However, the spectra contain fairly noisy backgrounds that could obscure less abundant ions, particularly at masses below 100.

Excluding losses of hydrogen atoms, the loss of a CH_n moiety generally gives rise to the base peak for the *protonated molecules* upon high-energy CAD (Figure 3). Loss of CH_2 from the protonated molecules can be pictured to occur via the reactions shown in Scheme I for the specific case of anthracene. The high product ion stability allows elimination of a high-enthalpy neutral molecule, CH_2. Loss of CH_n was found to be strongly dependent on the activation method used. Loss of CH_4, for example, is *not* usually observed upon electron ionization (Figure 2b), electron excitation, MPI (Figure 8), PD, or SIMS. On the other hand, high-energy CAD experiments result in abundant CH_n loss for all ions examined (see, for example, Figures 2–7). Low-energy collisional activation also causes CH_n to be lost.

Formation of $C_nH_2^+$ and $C_nH_3^+$. Two series of fragments, $C_nH_2^{\bullet+}$ (i.e., ions of m/z 38, 50, 62, 74, ...) and $C_nH_3^{\bullet+}$ (i.e., ions of m/z 39, 51, 63, 75, ...), are especially prominant at lower masses (n = 3–9) for EI (Figure 2b) and high-energy CAD (Figures 2a, 3, and 5). In the case of isomers, ions belonging to these series are of approximately equal abundance, making them of no value in isomer distinction. Examination of the CAD spectrum shown in Figure 2a reveals the presence of a $C_nH_2^{\bullet+}$ ion series extending from m/z 38 ($C_3H_2^{\bullet+}$) to m/z 146 ($C_{12}H_2^{\bullet+}$) in an unbroken sequence and having a maximum abundance for the ion of m/z 86 ($C_7H_2^{\bullet+}$). The same series of ions are observed for the sequential daughter spectra recorded for various fragment ions (Figures 5 and 6).

The sequential CAD spectra of $(M - 2H)^{\bullet+}$, $(M - 3H)^+$, and $(M - 4H)^{\bullet+}$ ions arising by dissociation of the chrysene molecular ion are shown in parts b–d of Figure 6. Each of the fragment ions, as well as the molecular ion itself (Figure 6a), loses CH_n and C_2H_n units and also forms the distinctive $C_nH_2^{\bullet+}$ ion series. However, the $C_nH_2^{\bullet+}$ ion series is of greater abundance for the hydrogen-poor parent ions (Figure 6b–d) than for the molecular ion (Figure 6a). A similar trend exists in the daughter spectra obtained for $(M - CH_2)^{\bullet+}$, $(M - CH_3)^+$, and $(M - CH_4)^{\bullet+}$ ions derived from fluorene (9) (supplementary material, Table V). The more hydrogen-poor the parent ion, the less facile the C_2H_n loss relative to the low-mass ion series (CH_n loss is not favored for these parent ions).

Formation of $C_nH_6^{\bullet+}$ and $C_nH_7^+$. The $C_nH_6^{\bullet+}$ ions (e.g., of m/z 126, 138, 150, 162, ...) and $C_nH_7^+$ ions (e.g., of m/z 127, 139, 151, 163, ...) are the most prominent ions with higher masses (n > 9) formed upon EI (Figure 2b) and high-energy CAD (Figures 2a and 3–6) as well as MPI (Figure 8). The ions belonging to these series, just as for those belonging to the $C_nH_2^{\bullet+}$ and $C_nH_3^+$ series, are formed with nearly identical abundances irrespective of the precursor ion. Low-energy CAD, electron excitation, and PD techniques do not yield spectra containing these series. For those cases where both the $C_nH_2^{\bullet+}/C_nH_3^+$ and $C_nH_6^{\bullet+}/C_nH_7^+$ series are observed, there is a minimum in the relative abundances of the fragment ions at the point where the $C_nH_2^{\bullet+}/C_nH_3^+$ ions give way to the $C_nH_6^{\bullet+}/C_nH_7^+$ ions (ca. in the m/z 130–150 region of the spectra; see, for example, Figure 2a).

Formation of Doubly Charged Ions. Doubly charged ions are only formed upon EI and high-energy CAD. Isomeric chrysene and naphthacene give very abundant doubly charged ions of m/z 113 and 114 corresponding to $(M - 2H)^{2+}$ and M^{2+}. The only truly distinguishing feature[5] between the fragmentation products of naphthacene and chrysene is the ratio in the abundance of the doubly charged ion of m/z 114 to that of m/z 113. Doubly charged ions corresponding to $(M - C_2H_2)^{2+}$ and $(M - C_2H_4)^{2+}$ are also observed.

An important source of structural information may lie in daughter spectra of doubly charged ions.[42,43] The structures of doubly charged ions derived from relatively simple aromatic molecules have been studied extensively. Kinetic energy release and appearance energy measurements suggest linear structures for small fragmenting doubly charged ions,[16,44,45] including the $C_nH_2^{2+}$ and $C_nH_6^{2+}$ series, whereas larger fragmenting ions may retain one or more rings.[17,18] Semiempirical MO calculations[46–49] indicate that not only the structures of the fragmenting $C_nH_2^{2+}$ ions but also the most stable structures of the nonfragmenting $C_nH_2^{2+}$ ions are linear. From available evidence, it appears that doubly charged molecular and fragment ions derived from PAHs have access to several isomeric forms, as has been suggested for doubly charged benzene.[17,18,44,50]

CAD spectra were obtained for doubly charged ions generated either by EI in the ion source or by stripping an electron from

---

(41) The fragments formed by successive hydrogen losses from the parent ion are not shown in all the figures and not listed in the tables (supplementary material), primarily because the mass region near the parent ion was not scanned in every case. The ions formed by hydrogen losses are considerably more abundant than other fragment ions (often ten times more abundant than those due to loss of CH_n or C_2H_n), making relative abundance values for the smaller ions difficult to comprehend. The parent ions are also excluded because usually only a small percentage (<10%) are converted to fragment ions.

(42) Cooks, R. G.; Beynon, J. H.; Ast, T. *J. Am. Chem. Soc.* **1972**, *94*, 1004.

(43) Cooks, R. G.; Ast, T.; Beynon, J. H. *Int. J. Mass Spectrom. Ion Phys.* **1973**, *11*, 490.

(44) Beynon, J. H.; Fontaine, A. E. *Chem. Commun.* **1965**, 717.

(45) Rabrenovic, M.; Beynon, J. H. *Int. J. Mass Spectrom. Ion Phys.* **1983**, *54*, 87.

(46) Jones, B. E.; Abbey, L. E.; Chatham, H. L.; Hanner, A. W.; Teleshefsky, L. A.; Burgess, E. M.; Moran, T. F. *Org. Mass Spectrom.* **1982**, *17*, 10.

(47) Pople, J. A.; Frisch, M. J.; Raghavachari, K.; von R. Schleyer, P. *J. Comput. Chem.* **1982**, *3*, 468.

(48) Appling, J. R.; Moran, T. F. *Chem. Phys. Lett.* **1985**, *118*, 188.

(49) Appling, J. R.; Shields, G. C.; Moran, T. F. *Org. Mass Spectrom.* **1986**, *21*, 69.

(50) Bentley, T. W.; Wellington, C. A. *Org. Mass Spectrom.* **1981**, *16*, 523.

the PAH molecular ions in a collision cell. Upon collision, the doubly charged ions may undergo dissociation either to two singly charged fragments or to a doubly charged ion and a neutral fragment. The most informative reactions from our point of view, however, are those where charge exchange occurs with the target gas and spontaneous dissociation of the singly charged PAH ion (dissociative charge exchange) follows. In Figure 7, the daughter spectrum of the doubly charged anthracene (7) molecular ion (178^{2+}) formed by charge stripping from the singly charged molecule ion (178^{+}) is compared with the daughter spectrum of the singly charged molecular ion generated by EI in the ion source. Singly charged fragment ions arising from the doubly charged ion can appear at m/z values above that of the parent doubly charged ion (m/z 89). These singly charged fragments (which arise by dissociative charge exchange[51]) are of very low abundance, but they are sufficiently abundant to identify their masses as being identical with those formed in the CAD of the singly charged parent ion. Ions of both the $C_nH_2^{\bullet+}$ and $C_nH_6^{\bullet+}$ series are clearly present. For all of the compounds studied, the fragments match those generated from singly charged parent ions. Daughter spectra of doubly charged molecular ions formed upon EI in the source show the same characteristics as the spectra of charge stripped ions. The fact that doubly charged ions after charge exchange fragment like singly charged ions suggests *a close structural similarity* between the two populations of fragmenting ions.

Discussion

Isomerization. The nearly identical fragmentation patterns obtained for different PAH isomers suggest extensive isomerization of many of the parent ions prior to dissociation. Ionized PAHs (and many of their fragment ions) have unusually high dissociation thresholds,[6,7,11] and, thus, some of the activated, non-decomposing ions may well have access to several isomeric forms.

For ions that fragment in the ion source, any preceding isomerization must be competitive with or faster than unimolecular decomposition. In MS/MS experiments, the parent ions selected for collisional activation are of lower energy than those that decompose in the ion source; in addition, they have the additional time required for transit from the source to the collision cell to isomerize prior to dissociation. The similarity between the EI and high-energy CAD spectra provides evidence that if such a slow isomerization takes place it leads mainly to the same products as the fast isomerization.

Further evidence for this argument is obtained from the finding that variation of the initial internal energy of ionized PAHs prior to excitation did not change the fragmentation patterns (the molecular ions were generated by 70- and 11-eV EI, as well as $CS_2^{\bullet+}$ charge exchange). Protonated molecules generated by isobutane CI have only 0.1–0.9-eV internal energy prior to activation in the collision chamber and thus are not likely to have enough internal energy to isomerize[52,53] yet their CAD spectra resemble those of activated radical cations. The same applies to PAH radical cations generated from radical anions. The stable $M^{\bullet-}$ ions cannot have high internal energies because the electron affinities of PAHs are less than 0.8 eV;[54] nevertheless, after conversion to positive ions in a rapid charge inversion process, these ions dissociate to give daughter spectra that are strikingly similar to those obtained for PAH cations.[13] All these results suggest that the isomerization responsible for the similarities in CAD and EI mass spectra of isomeric ions is fast enough to compete with direct dissociation *after excitation*. This is not to say, however, that the isomerization cannot occur also prior to activation in some stable ions of high internal energy which are preferentially sampled[55] upon collisional activation, nor does it imply that *all* dissociation products come from isomerized ions; this point will be addressed further in subsequent sections.

There is an additional consideration that has seldom been emphasized[56-58] and that is likely to enhance the degree of isomerization of PAHs after activation and prior to dissociation. As mentioned earlier, the lowest activation energy for dissociation of many PAH ions is unusually high. If the cross section for dissociation is much smaller than that for isomerization, collision conditions necessary to promote dissociation will correspond to several isomerizing collisions.

The minor but reproducible differences in the CAD spectra of *different ions* derived from the same PAH molecule occur mainly in the high-mass region. The marked preference to dissociate via the pathways leading to $(M - H_n)^+$ (n = 1–4), $(M - CH_n)^+$, and $(M - C_2H_n)^+$ ions suggests that there are *common reaction mechanisms* for ionic PAHs, perhaps involving a ring opening, that generate the same fragmenting units for each of the parent ions. This applies not only to fragment ions of different mass derived from the same PAH but also to ions derived from *different PAH molecules*.

Hydrogen loss from protonated PAH molecules takes place in the ion source as well as in the collision cell: when H_3^+ is used as a reagent to protonate PAH molecules, most of the resulting $(M + H)^+$ ions spontaneously lose $H^\bullet$. Isobutane reagent gas leads to more stable protonated molecules. The known hydrogen atom affinities of PAH molecular ions[59] indicate that 2.7–3.4 eV is needed to remove $H^\bullet$ from protonated PAHs. Thus, the exothermicity of proton transfer between H_3^+ (proton affinity of H_2 = 4.4 eV)[53] and, for example, anthracene (proton affinity = 9.1 eV) should be large enough (4.7 eV) to induce $H^\bullet$ loss, but the exothermicity of proton transfer with $C_4H_9^+$ reagent ion is not (proton affinity of C_4H_8 = 8.4 eV). The favored loss of $H^\bullet$ from protonated PAHs is testament to the inherent stability of PAH molecular ions. Supporting evidence comes from observations that many even-electron ions lose a radical, in violation of the "even-electron rule", to form ionized aromatic species.[60] For example, the dimethylstilbene molecular ion successively eliminates two methyl radicals to produce an abundant ion that formally corresponds to the phenanthrene molecular ion.[61]

Key Fragment Ions. Complete loss of structural identity takes place for those highly energized PAH parent ions that decompose to low mass fragments, such as those in the $C_nH_2^{\bullet+}$ and $C_nH_3^+$ series. The common feature of the low-mass region observed in high-energy CAD spectra of all ions derived from PAHs could be due to common intermediate species occurring along the major dissociation pathways. A common intermediate has been previously invoked to explain the similarity of the mass spectra of other aromatic isomers,[7] and of some unsaturated hydrocarbon ions at high activation energies.[62] For the compounds studied here, opening of at least one or two aromatic rings accompanied by hydrogen shifts is necessary to form a common structure. The singular pattern of low-mass peaks in the high-energy daughter ion spectra suggests the intermediacy of a large monocyclic or completely linear ion with cumulated double bonds along the length of the carbon chain. The gradual rise and fall of the peak intensities is similar to the pattern characteristic for 70-eV EI mass spectra of long-chain, linear aliphatic hydrocarbons.[63] Branched and cyclic molecules generally give spectra with a disruption in

---

(51) Charge separation probably does not occur to a significant extent, as indicated by the peak shapes (not flat or dished), and the absence of the expected complementary ions.

(52) Calculated by computing the differences in proton affinity between isobutene and various PAH. Data were taken from ref 53.

(53) Lias, S. G.; Liebman, J. F.; Levin, R. D. *J. Phys. Chem. Ref. Data* **1984**, *13*, 695.

(54) Buchanan, M. V.; Olerich, G. *Org. Mass Spectrom.* **1984**, *19*, 486.

(55) Cooks, R. G.; Beynon, J. H.; Litton, J. F. *Org. Mass Spectrom.* **1975**, *10*, 503.

(56) Cooks, R. G. In *Collision Spectroscopy*; Cooks, R. G., Ed.; Plenum Press: New York, 1978; p 357.

(57) (a) Kim, M. S. *Int. J. Mass Spectrom. Ion Phys.* **1983**, *50*, 189. (b) Kim, M. S. *Int. J. Mass Spectrom. Ion Phys.* **1983**, *51*, 279.

(58) Kenttämaa, H. I. *Org. Mass Spectrom.* **1985**, *20*, 703.

(59) Meot-Ner, M. *J. Phys. Chem.* **1980**, *84*, 2716.

(60) Karni, M.; Mandelbaum, A. *Org. Mass Spectrom.* **1980**, *15*, 53.

(61) Mintas, H.; Jakopcič, K.; Klasinc, L.; Güsten, H. *Org. Mass Spectrom.* **1977**, *12*, 544.

(62) Vainiotalo, P.; Kenttämaa, H. I.; Mabud, Md. A.; O'Lear, J. R.; Cooks, R. G. *J. Am. Chem. Soc.* **1987**, *109*, 3187.

(63) McLafferty, F. W. *Interpretation of Mass Spectra*, 3rd ed.; University Science: Mill Valley, CA, 1980; p 178.

the smooth pattern, with the location of the disruption depending upon the branching site. It should be noted that it may be possible, although entropically difficult, for some long-chain hydrocarbons to undergo the reverse process; in fact it has been suggested that cyclization of ionic C_9 diynes occurs upon fragmentation.[64] However, linear alkynes with more than six carbon atoms appear not to isomerize to cyclic forms.[65]

Further evidence for formation of linearized fragments from ionized PAHs comes from structural studies and energetic considerations based on appearance energies measured for various fragment ions of ionic phenanthrene (**8**) and naphthalene. It has been suggested that at least one ring opening takes place before or upon CH_n loss, and complete linearization probably occurs upon H_2 loss, whereas C_2H_n loss seems to take place from a structure with one intact aromatic ring.[7,11] Moreover, structures of $C_{10}H_6^+$ ions (m/z 126) formed by loss of two C_2H_2 units from ionized phenanthrene and diphenyl acetylene are claimed to be completely linear,[7] although inadequacies in the instrumentation available at the time of the study limit the value of this evidence.

Linearization of the ions studied probably takes place in a stepwise fashion in association with individual dissociation steps. This is supported by the dramatic changes observed for the low-mass CAD products of $M^{\bullet+}$, $(M - H)^+$, $(M - 2H)^{\bullet+}$, $(M - 3H)^+$, and $(M - 4H)^{\bullet+}$ ions (Figure 6; Table V in supplementary material). The relative abundances of these products increase as the number of dissociation steps required to generate the parent ion from the molecular ion increases [e.g., the relative abundances of the low-mass products increase in the order $M^{\bullet+} < (M - 2H)^{\bullet+} < (M - 3H)^+ < (M - 4H)^{\bullet+}$]. This suggests a stepwise change in the structure of the parent ion as its mass decreases. The fact that minor differences between the spectra of isomeric compounds can sometimes be detected in the high-mass region indicates that structural identity is maintained early in the dissociation scheme. The gap between the low-mass ion series and hydrogen-rich (high-mass) ions in high-energy daughter spectra of PAH (see also Figure 10) may represent the transition between fragments formed from common intermediates and cyclic precursors, respectively.

Literature data on structures of doubly charged PAHs suggest that the doubly charged ions also undergo stepwise ring openings upon dissociation. At least one ring opening, but probably not complete linearization, was concluded to precede or accompany the losses of CH_3^+, $C_2H_2^+$, and $C_3H_3^+$ from several doubly charged PAHs.[17] The smaller doubly charged fragment ions derived from PAHs, including $C_nH_6^{2+}$ and $C_nH_2^{2+}$ ions, have linear structures, and these structures are not dependent on the precursor molecule.[45-48] In the present work, it was found that the fragmentation behavior of charge-exchanged doubly charged molecular ions is similar to that of singly charged molecular ions generated by EI, which suggests that the structure(s) of the singly and doubly charged molecular ions are similar.

A candidate for one of the common intermediates in the fragmentation routes of PAHs is the ion $C_{12}H_6^{\bullet+}$ (m/z 150). In high-energy CAD, the low-mass ion series, $C_nH_3^+$ and $C_nH_2^{\bullet+}$, commonly become prominent just below mass 150. Collisional activation of $C_{12}H_6^{\bullet+}$, generated by CAD of the molecular ion of fluorene, produces the common low-mass ion series exclusively (double-collision experiment; Table V in supplementary material). This is not to suggest, however, that the m/z 150 ion is the *only* common intermediate, even for one particular compound.

The considerations just outlined suggest several structures for the key fragment ions observed in PAH spectra (Chart I). The cumulene structure, **a**, analogous to **b** (suggested in connection with doubly charged ions derived from PAH), may be a central intermediate. Its even-electron counterpart, **c**, accounts for the $C_nH_3^+$ series, whereas $C_nH_6^{\bullet+}$ (**d** and **e**), $C_nH_7^+$ (**f** and **g**), $C_nH_{10}^{\bullet+}$, and other abundant ions are also readily accommodated. Note that both odd and even numbers of carbon atoms are accommodated by the structures shown in Chart I.

Chart I

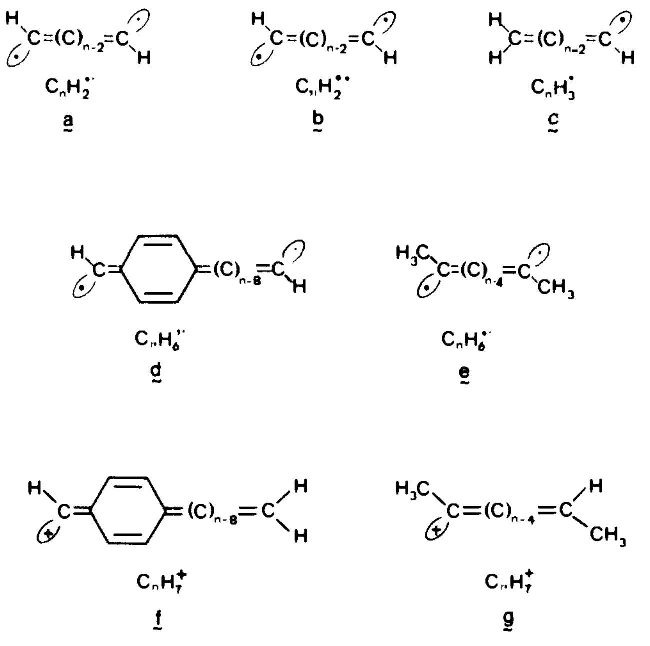

The isomerization mechanisms leading to these structures can be imagined as a retro-cyclization reaction. A compound such as pyrene has 10 carbon atoms that each carry a single hydrogen atom and 6 that carry none. Ring openings could lead to structures in which both cumulated and alternating double bonds occur. Hydrogen shifts and simple fragmentations (e.g., loss of C_2H_4 and C_2H_2) are proposed to lead to the key structures **a**–**g**.

Activation by Different Means. The differences in the extent of fragmentation obtained by using different activation methods can be explained in a straightforward manner. In studies of internal energy deposition,[30,66,67] it was demonstrated that an average energy of ca. 1–3 eV is deposited into an ion in a high-energy collision, but that the distribution of deposited energies exhibits a high-energy tail extending beyond 15 eV internal energy. Low-energy collisions, on the other hand, deposit low average energies to give distributions with *no* high-energy tail.[30,67] The maximum internal energy of an ion after a single low-energy collision has a cutoff approximately determined by the sum of the center-of-mass ion kinetic energy, E_{cm}, and the maximum internal energy of the ion prior to activation. This latter term corresponds to the activation energy, E_0, of the lowest energy fragmentation reaction. Fragmentations having activation energies greater than the cutoff value obtained by summing the two terms are not expected to occur upon low-energy collisions, but they may well take place after high-energy collisions.

The results for ionized phenanthrene (**8**) agree with these expectations.[30] The maximum calculated internal energy of a phenanthrene molecular ion after a single 28-eV collision with argon is approximately 13.6 eV ($E_0 + E_{cm} = 8.5 + 5.1$ eV). The major ionic fragments of ionized phenanthrene produced upon collision at 28 eV (Table IV in supplementary material) are ions of m/z 152, 151, 128, 139, and 163, arranged in decreasing order of abundance.[30] Neglecting the ion of m/z 128, for which no thermochemical data are available, all products have approximate activation energies for formation below the maximum internal energy of the activated molecular ion: 8.8, 11.8, 13.3, and 12.2 eV, respectively.[68] The lowest energy fragmentation produces the most abundant fragment—that yielding the ion of m/z 152. No fragments requiring very high activation energies are formed.

---

[64] Robbins, R. C.; Foster, N. G. Presented at the 33rd Annual Conference on Mass Spectrometry and Allied Topics, San Diego, 1985.

[65] Wagner-Redeker, W.; Levsen, K.; Schwarz, H.; Zummack, W. *Org. Mass Spectrom.* **1981**, *16*, 361.

[66] Kim, M. S.; McLafferty, F. W. *J. Am. Chem. Soc.* **1978**, *100*, 3279.

[67] Kenttämaa, H. I.; Cooks, R. G. *Int. J. Mass Spectrom. Ion Proc.* **1985**, *64*, 79.

[68] Rosenstock, H. M.; Draxl, K.; Steiner, B. W.; Herron, J. T. *J. Phys. Chem. Ref. Data* **1977**, *6*, Suppl. 1.

In contrast, the high-energy CAD spectrum (Table III in supplementary material) shows the presence of numerous low-mass ions that are presumably formed as a result of high internal energies (>15 eV) being deposited in the parent ions in the high-energy collisions.[30] A noteworthy point is that peak groups due to ions with differing numbers of hydrogens are present in the high-energy CAD spectrum (e.g., *m/z* 150, 151, 152) but are absent in the low-energy CAD spectrum (*m/z* 152 only). This can be rationalized on the basis of a low probability, in low-energy CAD, for depositing the high internal energies that are required for formation of ions of *m/z* 150 and 151, but a high probability for depositing the smaller amount of energy that is necessary to form the ion of *m/z* 152. In fact, this probability may be higher for low-energy CAD than for high-energy CAD, as the products obtained for phenanthrene suggest (formation of the ion of *m/z* 152 is not as favored upon high-energy CAD as upon low-energy CAD).

The observation of favored CH_n losses for only some of the activation methods requires further explanation. CH_n losses are prominent for low-energy as well as for high-energy CAD of all the singly and doubly charged ionized PAHs studied. The corresponding product ions are somewhat less abundant for low-energy CAD than for high-energy CAD, presumably because of the high-energy requirements of these fragmentations (about 12 eV for phenanthrene).[30] In contrast, ions formed by losses of CH_n units are minor or absent upon EI, MPI,[69] SIMS, and photodissociation of PAHs. For these methods, fragmentation takes place either in the ion source, where the residence time is usually less than a microsecond, or in the cell of the FTMS, where the ion residence time is longer than several milliseconds.

The high-energy requirements for loss of CH_n may explain the absence of the product ions in MPI, SIMS, and photodissociation, but the requirements do not account for its absence in EI. Invoking different forms of energy initially deposited in the ions also is not an explanation for the appearance of CH_n losses in CAD and the absence of these losses in EI, because CH_n units are lost independently of whether the parent ions are initially electronically (high-energy CAD, EI, MPI) or vibrationally (low-energy CAD) excited. A possible explanation is that the shapes of the internal energy distribution curves [$P(E)$ versus E] in EI and high-energy CAD are different in the critical range; CH_n loss may occur at energies where there is a low probability for producing ions by EI. This is difficult to prove although a related explanation has been shown to account for anomalous behavior in other compounds, notably retro-Diels–Alder fragmentation of limonene.[70] A more likely possibility is that several excitation steps—as opposed to the single-step excitation common in EI—are necessary to induce CH_n loss. In other words, the isomer(s) from which this loss occurs is relatively inaccessible, and consecutive excitation by energy deposition upon ionization followed by collisional activation, or by several collisions in the collision region, may assist in reaching the reactive configuration.[58,71]

The observation that collision-induced CH_n losses appear to be generally more favorable for the protonated PAH molecules than for the molecular ions can be explained by the fact that the loss of CH_2 or $CH_3^{\bullet}$ from the protonated molecules does not require as extensive a preceding isomerization as is necessary for the molecular ions.

Summary of the Fragmentation Pathways. A simplified diagram based on the known thermochemistry of phenanthrene and anthracene is shown in Figure 9 to illustrate the general behavior of activated ions derived from PAHs. The diagram summarizes the factors that underlie the variety of observations made in the present study. Note that the key points are these: (i) there are fragment ions that are common intermediates in the dissociation of parent ions derived from isomeric or completely different molecules and/or representing different types ($M^{\bullet+}$, $(M - H_n)^+$, $(M - CH_n)^+$, etc.); (ii) these intermediates are generated by a combination of isomerization and dissociation reactions involving losses of common neutral fragments; (iii) ion series composed of structures with cumulated double bonds and none or only a few rings appear to be the ultimate products of fragmentation of all ions derived from PAH.

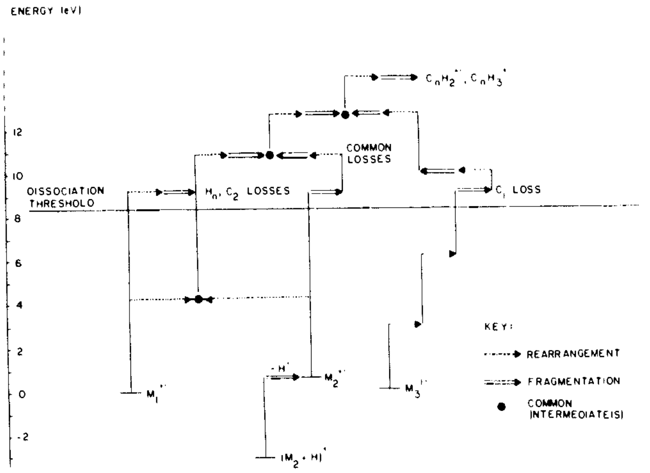

Figure 9. Hypothetical energy diagram illustrating the major aspects of the mass spectrometric behavior of PAHs. M_1 and M_2 are isomers, while M_3 is a molecule of different molecular weight. In addition to other processes not shown, each of the specific fragmentation types illustrated for the molecular ions (H losses, C_2 loss, C_1 loss) takes place for each of the parent ions, i.e., M_1 and M_2 lose C_1 units (probably preceded by isomerization of the molecular ion) in addition to the $H^{\bullet}$, H_n, and C_2 losses indicted, and M_3 loses $H^{\bullet}$ (which presumably occurs from a non-isomerized structure) in competition with C_1 loss, etc. A combination of isomerization and fragmentation reactions results in common intermediates for different molecular ions and different fragment ions, which then lead to common ion series. Lengths and numbers of arrows are merely illustrative. The relative energies are based on the known thermochemistry of phenanthrene and anthracene as far as possible, but they should be considered directive only.

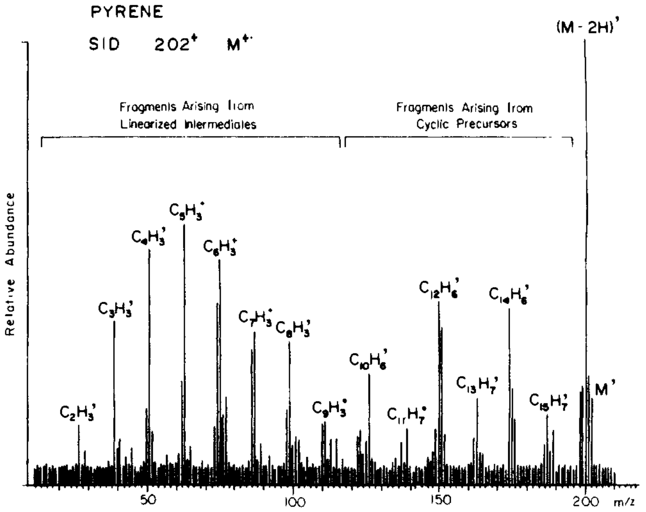

Figure 10. Daughter spectrum obtained[69] by allowing pyrene molecular ions to collide with a surface at 100 eV collision energy.

These concepts are exemplified by the surface-induced dissociation (SID) spectrum of pyrene (6). In SID, a large amount of internal energy can be deposited into an ion,[22,36] and the 100-eV SID spectrum of the pyrene molecular ion (Figure 10) bears this out. Two separate regions due to hydrogen-rich high-mass and hydrogen-poor low-mass ions are apparent, as is the case for

---

(69) Lubman, D. M.; Naaman, R.; Zre, R. N. *J. Chem. Phys.* **1980**, *72*, 3034.

(70) Vincenti, M.; Horning, S. R.; Cooks, R. G. *Org. Mass Spectrom.*, in press.

(71) Spectra of metastable PAH ions were obtained earlier by B/E linked scans and show low-intensity peaks due to C_1 losses.[10,11] It is possible, however, that pressures were not sufficiently low in these studies to invalidate the stepwise excitation hypothesis, particularly in view of the fact that the fragmentations had to occur near the ion source in the first field-free region of the mass spectrometer.

(72) Bier, M. E.; Amy, J. W.; Cooks, R. G.; Syka, J. E. P.; Ceja, P.; Stafford, G. *Int. J. Mass Spectrom. Ion Proc.* **1987**, *77*, 31.

high-energy CAD spectra of PAH ions. The hydrogen-rich ions, which are mainly of the type $C_nH_6^{\bullet+}$ and $C_nH_7^+$, probably arise from largely cyclic precursors and are themselves probably linear. In contrast, the hydrogen-poor ions ($C_nH_2^{\bullet+}$ and $C_nH_3^+$) presumably arise from further fragmentation of the more hydrogen-rich linearized intermediates.

Conclusions

(i) Differences in the internal energy distributions of ions excited by various means are the chief factors controlling the spectral features of PAHs. Only activation methods that can deposit very high energies (e.g., high-energy collisional activation, surface-induced dissociation) cause extensive dissociation of ionized PAH because of the extraordinarily high activation energies for dissociation of these ions.

(ii) The remarkable stability of the parent ions increases the probability of multistep excitation. Isomerization induced by multistep excitation of the parent ions may explain the appearance of products from CH_n losses, particularly evident in collisional activation.

(iii) The dramatic similarity of the dissociation product distributions obtained for different ions derived from PAH, especially the loss of common small neutral fragments and the identical low-mass regions of the spectra, can be explained as follows: after activation, the various fragmenting parent ions rearrange by ring opening to form the same fragmenting structural units for each of the parent ions (this leads to isomerization in the case of closely related structures). Fragmentation by loss of common small neutral fragments finally leads to formation of common intermediate fragment ions which produce the low-mass fragmentation products common for all PAH parent ions. Partial isomerization of some parent ions prior to activation cannot be excluded.

(iv) Because the basic reasons for obtaining similar dissociation products for different parent ions are intrinsic to the dissociation mechanisms (see iii), the use of different excitation methods or experimental conditions will not facilitate isomer differentiation. However, doubly charged and singly charged ions that have lost no carbon units can sometimes aid in distinguishing isomers, because partial or complete structural integrity is retained in these cases.

Acknowledgment. This work was supported by the National Science Foundation (Grant CHE-8408258), the donors of the Petroleum Research Fund, administed by the American Chemical Society, and the Midwest Center for Mass Spectrometry, an NSF regional instrumentation facility (Grants CHE-8211164 and CHE-8320388). S.J.P. thanks the Dow Chemical Co. for a graduate fellowship through the Purdue Industrial Associates Program. H.I.K. thanks the Academy of Finland for a fellowship.

Registry No. 1, 50-32-8; **2**, 192-97-2; **3**, 92-24-0; **4**, 218-01-9; **5**, 206-44-0; **6**, 129-00-0; **7**, 120-12-7; **8**, 85-01-8; **9**, 86-73-7.

Supplementary Material Available: 70 eV electron ionization mass spectra of PAHs (Table II), high-energy CAD spectra of PAHs (Table III), low-energy CAD daughter spectra of PAHs (Table IV), high-energy sequential daughter spectra of PAHs (Table V), high-energy CAD spectra of doubly charged PAH ions (Table VI), and SIMS spectra of PAHs supported on silver (Table VII) (11 pages). Ordering information is given on any current masthead page.